Comprehensive Characterization and Electrochemical Analysis of Zinc-Doped Manganese Ferrite Nanoparticles: Potential for Supercapacitor Applications

Section A-Research paper

Comprehensive Characterization and Electrochemical Analysis of Zinc-Doped Manganese Ferrite Nanoparticles: Potential for Supercapacitor Applications

Abisha.D [a,e], Gibin.S.R [b,e,*], PremKumarV.K [c], Rajeevgandhi[d]

[a]Reg.No:20113082132012, Research Scholar, Department of Physics and Research Centre, Malankara Catholic College, Mariagiri, Kaliakkavilai-629153, Tamil Nadu, India.

[b]Department of Physics and Research Centre, Malankara Catholic College, Mariagiri, Kaliakkavilai-629153, Tamil Nadu, India.

[c]Laboratory of Electrochemical Energy Storage, Institute of Environmental Resources Engineering Zhejiang University China.

[d]Department of physics, Sri Indu college of Engineering and Technology, Ibrahimpatan, Telugana-501510 India
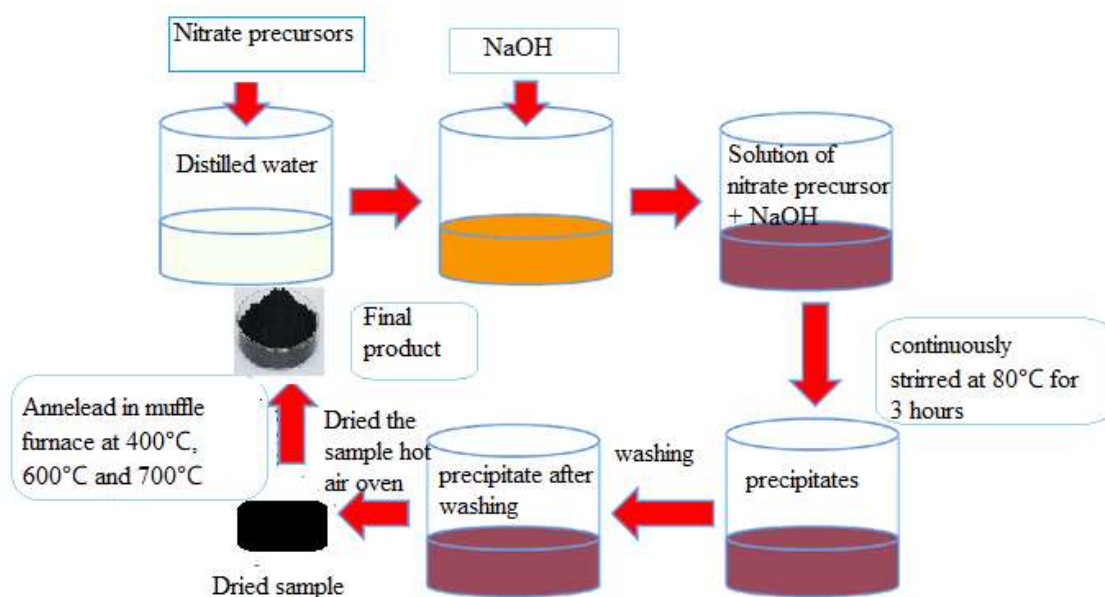
[e]Affiliated to Manonmaniam Sundaranar University, Abishekapatti-627012, Tirunelveli, Tamil Nadu, India

Abstract:

Zinc-doped manganese ferrite nanoparticles were synthesized using the co-precipitation technique and subsequently annealed at different temperatures ($400°C$, $600°C$, and $700°C$). The synthesized samples underwent characterization using several techniques including TG/DTA, XRD, FTIR, SEM, TEM, EDX, XPS, BET, and CV. The sample's thermal behaviour and decomposition were examined using differential thermal analysis and thermo gravimetric analysis. The crystal structure and phase purity of the nanoparticles were examined using X-ray diffraction (XRD). Fourier transform infrared spectroscopy was used to identify the chemical bonds present in the samples. The surface morphology and particle size of the $Mn_{0.5}Zn_{0.5}Fe_2O_4$ nanoparticles, annealed at $700°C$, were investigated using scanning electron microscopy and High- Resolution transmission electron microscopy with selected area electron diffraction patterns providing crystal structure and orientation information. Energy dispersive X-ray spectroscopy (EDX) analysis confirmed the presence of manganese, zinc, iron, and oxygen in the synthesized nanoparticles. The specific surface area of the samples was examined using the Brunauer-Emmett-Teller method, providing insights into nanoparticle porosity and surface characteristics. X-ray photoelectron spectroscopy was utilized to measure the binding energy of the samples, yielding information about their electronic structure and chemical composition. Cyclic voltammetry (CV) was employed to analyze the electrochemical properties of the samples, revealing a specific capacitance value of 388.35 Fg^{-1} at a lower scan rate of $2mVs^{-1}$. This high specific capacitance suggests the potential suitability of $Mn_{0.5}Zn_{0.5}Fe_2O_4$ nanoparticles for supercapacitor applications.

Keywords: Co-precipitation, Surface morphology, particle size, supercapacitor.

96

Eur. Chem. Bull. 2022, 11 (01), 96 – 115

Comprehensive Characterization and Electrochemical Analysis of Zinc-Doped Manganese Ferrite Nanoparticles: Potential for Supercapacitor Applications

Section A-Research paper

Graphical Abstract

*Corresponding author:

Gibin.S.R

Department of Physics and Research Centre,

Malankara Catholic College, Mariagiri,

Kaliakkavilai-629153, Tamil Nadu, India.

E-mail. gibin.physics@gmail.com

Mob: 9894469432

Introduction:

The potential uses of magnetic nanoparticles in a variety of fields, particularly high-temperature magnetic refrigeration, high-density information storage, medical diagnosis, color imaging and electromagnetic wave absorption, have generated a great deal of interest [1]. Manganese zinc ferrite, known for its remarkable electromagnetic properties, chemical stability, corrosion resistance, and affordability, has been extensively investigated [2].

The characterization and use of manganese zinc ferrite nanoparticles, particularly for magnetic data storage technology and biological applications, have attracted more attention over the past few years. Manganese zinc ferrites belong to the category of soft magnetic materials known for their exceptional magnetic penetration capabilities [3]. Soft ferromagnetic materials like manganese, nickel, and copper ferrites exhibit advantageous characteristics such as high resistivity, high initial permeability, high dielectric constant, low power losses and high saturation magnetization. By introducing particular transition metal ions into the spinel structure of ferrites, numerous cations can migrate across lattice sites. This directly affects the ferrite's essential features, especially their magnetic behaviour [4].

Due to its important magnetic and electrical properties, zinc ferrite has been widely used in a variety of commercial applications, including absorbent materials, photocatalysts, gas sensors, catalysts, magnetic resonance imaging (MRI), and Li-ion batteries [5]. The

97

Comprehensive Characterization and Electrochemical Analysis of Zinc-Doped Manganese Ferrite Nanoparticles: Potential for Supercapacitor Applications

Section A-Research paper

incorporation of dopants plays a crucial role in altering the elastic properties of these nanocrystals. The introduction of different impurities induces defects in the crystal structure and texture, leading to significant modifications in key material properties, particularly the elastic properties. Extensive investigations have been conducted to incorporate different dopants into ferrites (Fe_2O_4) to explore the magnetic and electrical properties of these materials. Various synthesis methods, including hydrothermal techniques, sol-gel methods, microwave emulsion processes, and co-precipitation methods, have been employed to fabricate ferrites. Comparatively, the co-precipitation method offers advantages such as simplicity, cost-effectiveness, and precise control over particle size and purity. Nanoparticles exhibit distinct properties from their bulk counterparts due to their large surface-to-volume ratio, which introduces surface effects. In the case of ferrite nanoparticles, intriguing magnetic phenomena can arise, including superparamagnetism, spin canting, core-shell structures, reduction in saturation magnetization, and the presence of single-domain characteristics [6].

Mn-Zn ferrites retain their status as magnetic materials of significant importance, finding wide-ranging applications in everyday life, production technology, scientific research, and national defense [7]. Extensive research has been conducted to investigate the intriguing magnetic and electromagnetic properties of Mn-Zn ferrites, owing to their exceptional attributes. These ferrites exhibit favourable chemical stability, magnetic properties, and cost-effectiveness [8].

The co-precipitation method was employed to synthesize zinc-doped manganese ferrite nanoparticles. The synthesis process involved combining manganese, zinc, ferric compounds, citric acid, and sodium hydroxide in a 1:2:3 ratio. The resulting mixture was subjected to annealing at temperatures of 400°C, 600°C, and 700°C for 3 hours. Following annealing, the sample was ground into a powder using a mortar and pestle. The powdered sample underwent a comprehensive characterization process using various analytical techniques. Thermo gravimetric analysis and Differential thermal analysis, X-ray diffraction, Scanning electron microscopy, High-resolution transmission electron microscopy, cyclic voltammetry, Brunauer-Emmett-Teller analysis, Fourier-transform infrared spectroscopy, Energy dispersive X-ray analysis, and X-ray photoelectron spectroscopy were employed. These characterization techniques allowed for the examination of thermal behaviour, crystal structure, surface morphology, electrochemical properties, specific surface area, chemical composition, and binding energies of the synthesized zinc-doped manganese ferrite nanoparticle sample.

2. Materials and method:

2.1 Synthesis of $Mn_{0.5}Zn_{0.5}Fe_2O_4$ nanoparticle:

Nano-crystalline $Mn_{0.5}Zn_{0.5}Fe_2O_4$ nanoparticles were successfully synthesized using a co-precipitation technique. The chemical reagents, obtained from Merck Chemicals, were directly used without any additional purification. The synthesis of $Mn_{0.5}Zn_{0.5}Fe_2O_4$ nanoparticles 0.5M $Mn(NO_3)_2 \cdot 4H_2O$, 0.5M $Zn(NO_3)_2 \cdot 6H_2O$, 0.2 $Fe(NO_3)_2 \cdot 9H_2O$ and 0.29 M of citric acid ($C_6H_8O_7$) were dissolved in 20ml of deionized water individually. Afterward, the solution was added one by one respectively with stirring continuously at 650 rpm. The precipitating agent was diluted with sodium hydroxide to the proper concentration. The

98

Comprehensive Characterization and Electrochemical Analysis of Zinc-Doped Manganese Ferrite Nanoparticles: Potential for Supercapacitor Applications

Section A-Research paper

dissolved solution was then agitated at 80°C for three hours. After a dark brown precipitate formed, it was extensively cleaned using acetone and deionized water many times. Then the precipitate was dried in the oven to form $Mn_{0.5}Zn_{0.5}Fe_2O_4$ powder and then it was annealed at different temperatures such as 400℃, 600℃ and 700℃.

2.2 Characterization:

The crystalline phase of the $Mn_{0.5}Zn_{0.5}Fe_2O_4$ nanoparticles was examined through X-ray diffraction analysis using a BRUKER USA D8 Advance, Davinci instrument. CuKα radiation with a wavelength of 1.54060Å was employed, operating at 40 kV and 30 mA. At a scan speed of 10°/min, step scans were recorded in the 2 range of 20° to 80°. Phase identification was carried out by referencing the International Centre for Diffraction Data database. The degradation behaviour of the synthesized sample was evaluated using thermal gravimetric and differential thermal analysis performed on a NETZSCH-STA 449 F3 JUPITER instrument. Fourier transform infrared spectroscopy was conducted using a Purkin-Elmer model Spectrum Two to analyze the chemical bonds present in the sample. For characterization purposes, scanning electron microscopy was performed using a CAREL ZEISS EVO 18 model after sputtering the sample. Additionally, a High-Resolution transmission electron microscope coupled with Energy dispersive X-ray spectroscopy was utilized. The HR-TEM analysis was conducted using an FEI-TECNAI G2-20 TWIN model operating at 200kV to investigate the morphology and determine the particle size. Elemental analysis was carried out using Energy dispersive X-ray spectroscopy with a Bruker EDX instrument equipped with an LN2-free detector. The selected area electron diffraction pattern was obtained by depositing the sample onto a carbon-coated copper grid. X-ray photoelectron spectroscopy measurements were performed using a ULVAC-PH1 INC model PH150000 version probe 111 to examine the elemental composition and chemical states of the sample. The Brunauer-Emmett-Teller method, utilizing a Quantachrome Instruments Autosorb IQ series, was employed to investigate the nanoparticle's pore size and surface area. To assess the electrochemical properties, cyclic voltammetry (CV) experiments were conducted using a Versa STAT MC model.

3. Result and Discussion:

3.1. Thermo Gravimetric and Differential Thermal Analysis (TG/DTA):

Fig 1 indicates the TG (Thermo Gravimetric) and DT (Differential Thermal) analysis curves obtained from the thermal analysis study conducted on the prepared $Mn_{0.5}Zn_{0.5}Fe_2O_4$ sample. These curves provide valuable information about the temperature at which transformations or changes occur within the sample.

99

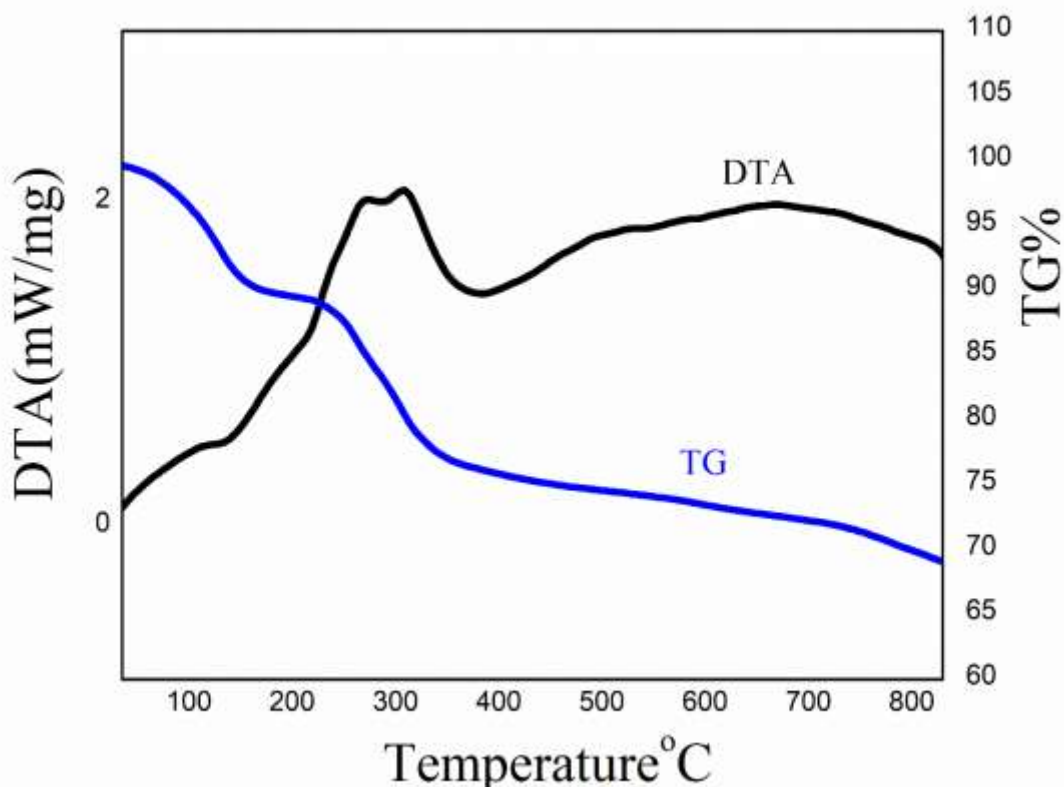Eur. Chem. Bull. 2022, 11 (01), 96 – 115

Comprehensive Characterization and Electrochemical Analysis of Zinc-Doped Manganese Ferrite Nanoparticles: Potential for Supercapacitor Applications

Section A-Research paper

Fig 1. TG/DT analysis curve of $Mn_{0.5}Zn_{0.5}Fe_2O_4$

The temperature range for thermo gravimetric evolution was found to be 35℃ to 850℃ [9]. Analysis of the TG-DT curves indicated that the sample underwent water desorption, breakdown of metal hydroxides, and the production of spinel ferrite. The TG curve exhibited three distinct weight losses, while the DT curve showed two endothermic and one exothermic peak corresponding to each weight loss [10].

During the first stage, occurring from 35℃ to 190℃, a moderate weight loss of 10% was observed, primarily attributed to water molecule desorption. The second stage, spanning 190℃ to 350℃, displayed a significant weight loss of 16% due to the decomposition of nitrates and other organic templates. In the third stage, between 350℃ and 600℃, a minor weight loss of 4% occurred as a result of the sample's phase transition. Beyond 600℃, no further weight losses were observed, indicating the formation of spinel ferrite nanoparticles [11].

The DTA curve showed an endothermic peak at 140°C and 380°C, which is suggesting of dehydration [12] [13]. Additionally, an exothermic peak was observed at 310℃, indicating the decomposition of residual nitrate ions [14].

3.2. X-Ray Diffraction (XRD):

The X-ray diffraction pattern illustrates the structural analysis of zinc-doped manganese ferrite nanoparticles synthesized through the chemical co-precipitation method. The samples were subjected to annealing at 400℃, 600℃, and 700℃. XRD is a useful method that is frequently used to analyse the crystal structure of materials, especially in the context of various crystalline nanomaterials, as well as to calculate the average crystallite size of the

100

Eur. Chem. Bull. 2022, 11 (01), 96 – 115

Comprehensive Characterization and Electrochemical Analysis of Zinc-Doped Manganese Ferrite Nanoparticles: Potential for Supercapacitor Applications

Section A-Research paper

synthesized sample. [15]. Fig 2 presents the XRD pattern specifically for $Mn_{0.5}Zn_{0.5}Fe_2O_4$, providing valuable information about its structural characteristics.
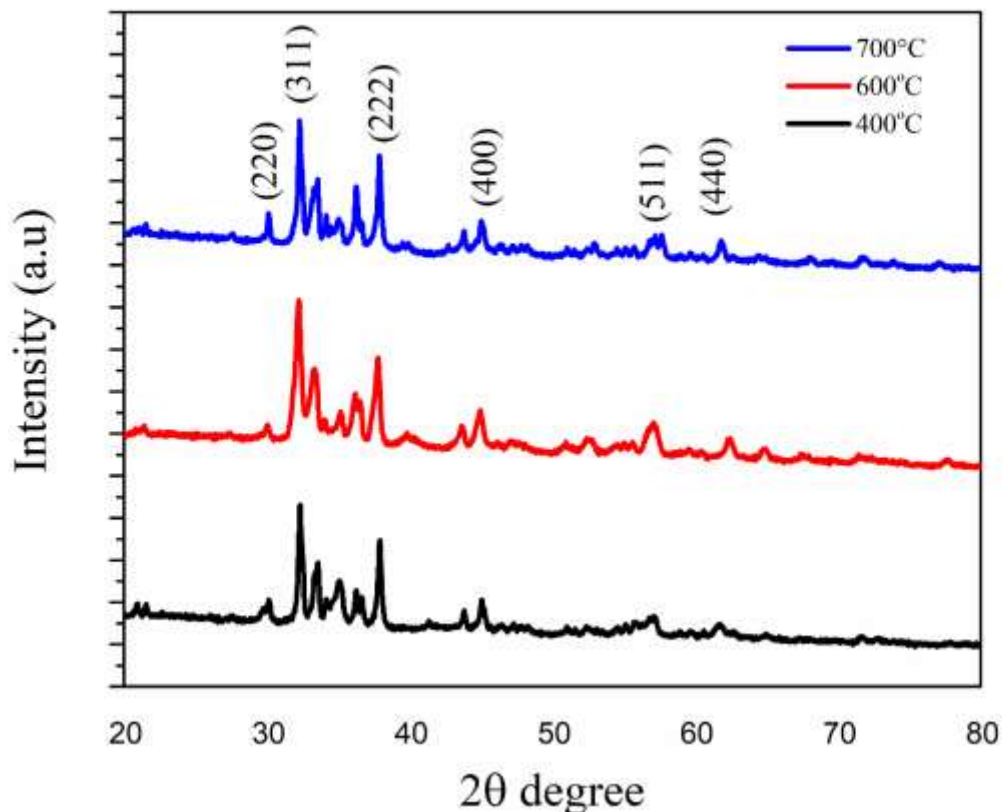

Fig 2. XRD pattern for $Mn_{0.5}Zn_{0.5}Fe_2O_4$

   The XRD analysis revealed diffraction peaks at 2θ values of 30.00°, 32.301°, 36.24°, 45.09°, 57.43°, and 61.90°, corresponding to the crystallographic planes (220), (311), (222), (400), (511), and (440), respectively. These diffraction peaks demonstrate the highly crystalline nature of the sample. The XRD peaks were matched with the standard reference patterns for $MnFe_2O_4$ (ICDD Card no 00-010-0319) [16] [17] and $ZnFe_2O_4$ (ICDD Card no 01-079-1150) [18], confirming the sample's purity. Additionally, it was found that annealing caused the diffraction peaks to become narrower and sharper, suggesting an increase in particle size. Using Debye-Scherrer's equation, the prepared sample's average particle size was calculated [19].

$$D = \frac{K\lambda}{\beta Cos\theta}$$

   Here, the crystalline size (D) in nanometers (nm) with various factors. The diffraction constant (k), which is typically around 0.9 and accounts for the shape factor, is used in the equation. The wavelength of the incident X-ray (λ), the calculated value of β based on the full width at half maximum of the diffraction peak, and the diffraction angle (θ) are also taken into consideration. Applying equation (1), the average crystalline size of the synthesized samples was estimated to be found 50 nm [20].

101

Eur. Chem. Bull. 2022, 11 (01), 96 – 115

Comprehensive Characterization and Electrochemical Analysis of Zinc-Doped Manganese Ferrite Nanoparticles: Potential for Supercapacitor Applications

Section A-Research paper

3.3. Fourier Transform Infrared Spectroscopy (FTIR):

The FTIR spectra of $Mn_{0.5}Zn_{0.5}Fe_2O_4$, displayed in Fig 3, cover the spectral range of 400 - 4000 cm^{-1}. Below 1000 cm^{-1}, an absorption peak signifies the presence of ferrites. In the FTIR spectra of the ferrite, two distinct absorption bands can be identified. The lower band, located at 459.82 cm^{-1}, corresponds to the metal ion-oxygen complex in the octahedral sites, while the higher band at 553.07 cm^{-1} indicates the metal ion-oxygen complex in the tetrahedral sites [21]. Additional peaks in the FTIR spectrum include the stretching vibrations of C-H and C=O bonds, appearing at 2956.59 cm^{-1} and 1643.98 cm^{-1}, respectively. The absorption peak at 1436.36 cm^{-1} is attributed to the bending vibration of the C-H group [22]. Moreover, vibrations associated with the C-C ring and C-N=O bending are evidenced by peaks at 866.27 cm^{-1} and 672.72 cm^{-1}, respectively [23].
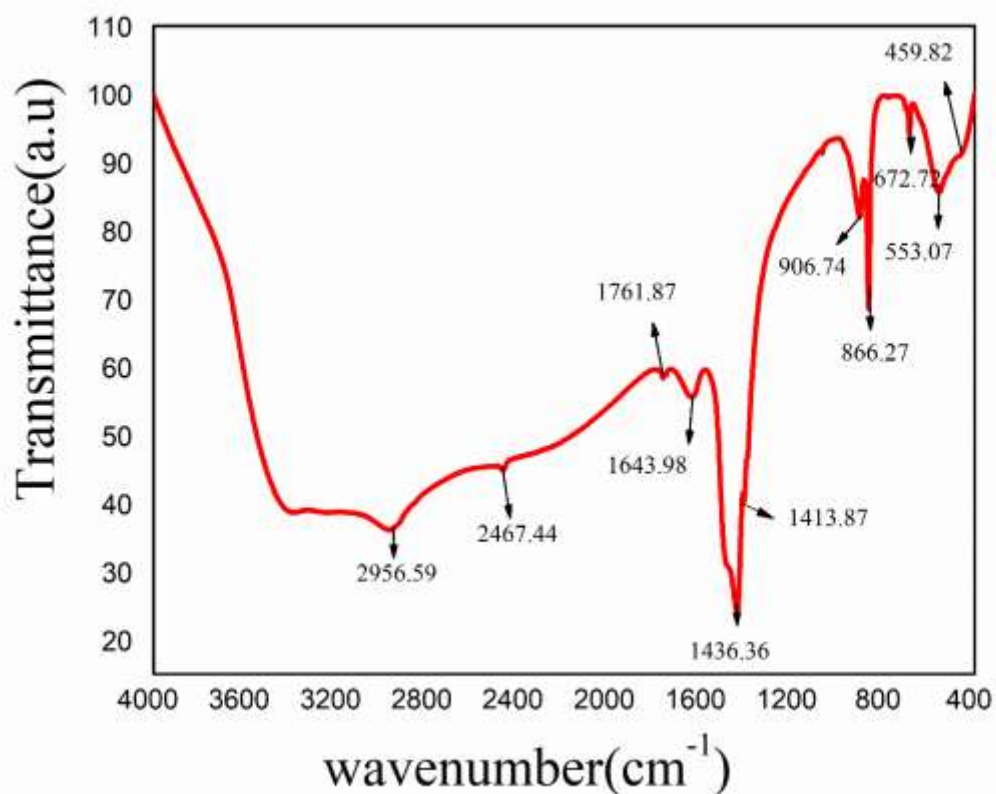

Fig 3. FTIR spectra of $Mn_{0.5}Zn_{0.5}Fe_2O_4$

102

Eur. Chem. Bull. 2022, 11 (01), 96 – 115

Comprehensive Characterization and Electrochemical Analysis of Zinc-Doped Manganese Ferrite Nanoparticles: Potential for Supercapacitor Applications

Section A-Research paper

3.4 Scanning Electron Microscope (SEM):

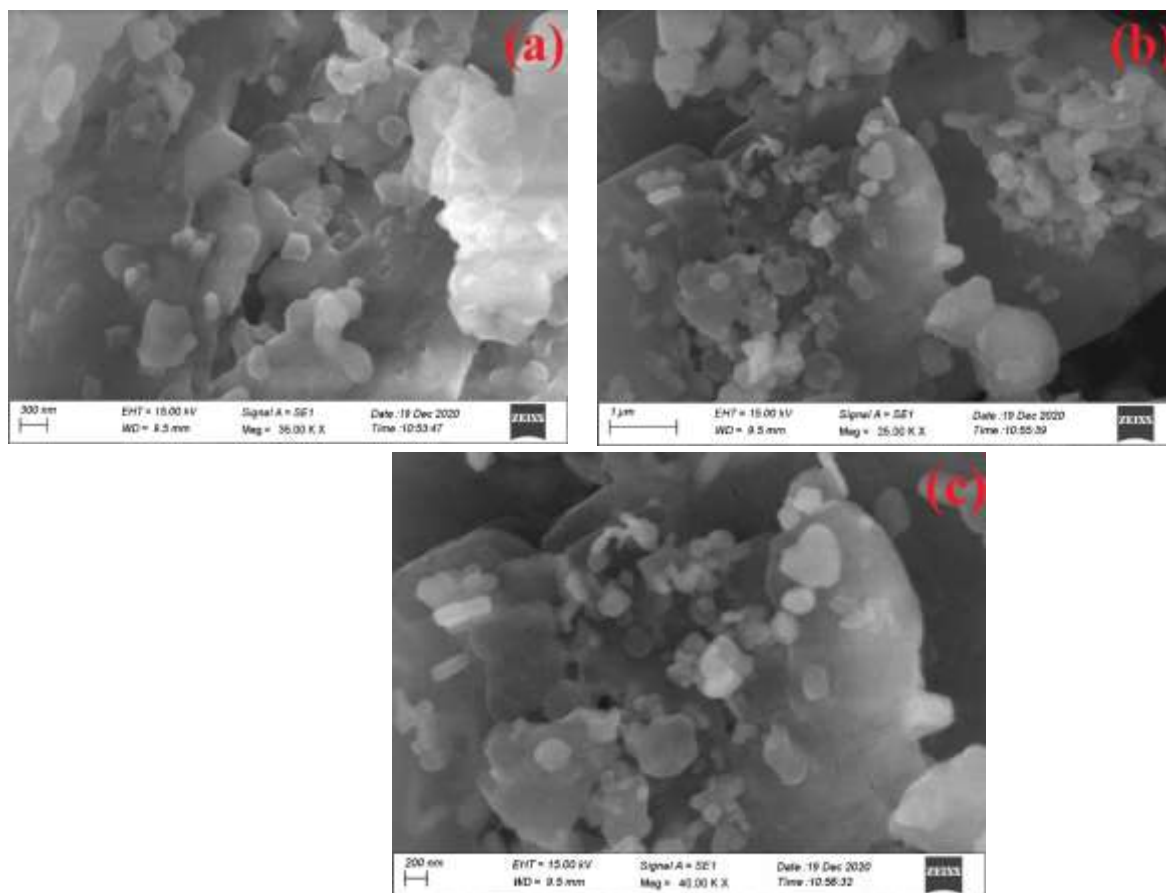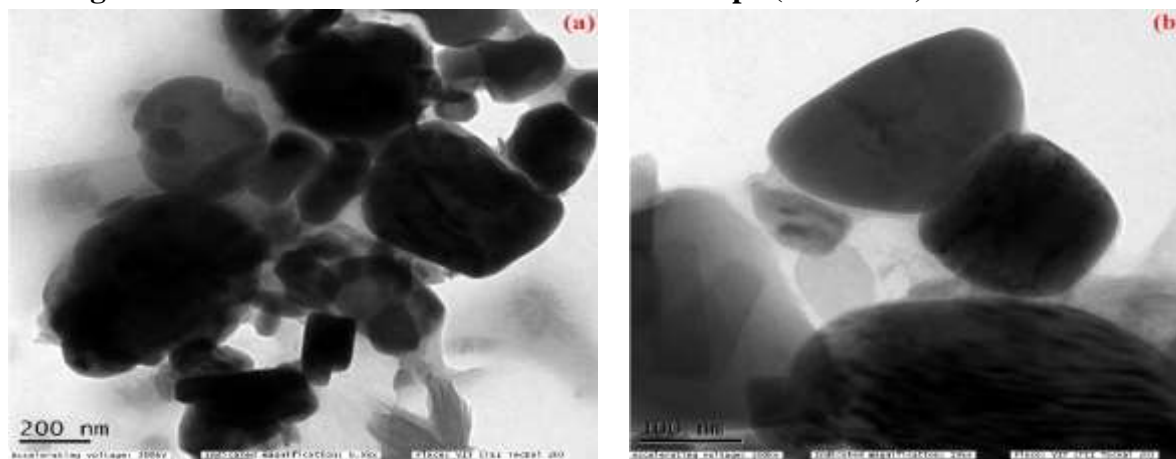**Fig 4 (a), (b) and (c) SEM image of $Mn_{0.5}Zn_{0.5}Fe_2O_4$ annealed at 700℃**

The manganese zinc ferrite nanoparticles' morphology was examined using scanning electron microscopy. Fig 4 (a), (b), and (c) present the SEM images of the sample, demonstrating its morphology annealed at 700℃. The microstructure of the grain sample displays a mixture of roughly spherical shape with agglomeration [24].

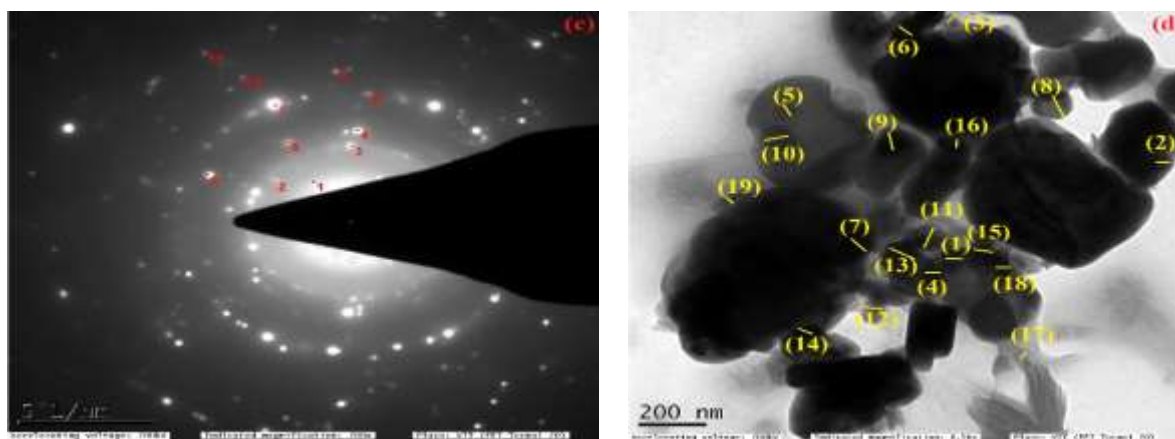**3.5 High-Resolution Transmission Electron Microscope (HR-TEM):**

103

Eur. Chem. Bull. 2022, 11 (01), 96 – 115

Comprehensive Characterization and Electrochemical Analysis of Zinc-Doped Manganese Ferrite Nanoparticles: Potential for Supercapacitor Applications

Section A-Research paper

Fig 5 (a), (b) HR-TEM of $Mn_{0.5}Zn_{0.5}Fe_2O_4$ nanoparticle annealed at 700℃ with different magnifications, and (c) shows the SAED pattern, (d) particle size measured using image 'j' viewer software.

The High-Resolution Transmission Electron Microscope was utilized to investigate the particle size and nanostructure of zinc-doped manganese ferrite nanoparticles after annealing at 700℃. Fig 5(a-d) displays the HR-TEM images obtained. In Fig 5(a) and (b), different scale bars of 100 and 200 nm are shown, providing a clear view of the morphology of $Mn_{0.5}Zn_{0.5}Fe_2O_4$ nanoparticles. The images reveal variations in particle size and shape, confirming the characteristics of the ferrite particles [25].

The observed agglomerated particles in Fig 5(a) and (b) exhibit a roughly spherical shape for $Mn_{0.5}Zn_{0.5}Fe_2O_4$ nanoparticles. Using the "Image J Viewer" software, the average particle sizes were calculated and determined to be in the range of 48 nm [26], which is identical to the results of the XRD analysis. The Selected Area Electron Diffraction pattern depicted in Fig 5(c) displays concentric rings around spots, indicating the polycrystalline nature of the synthesized $Mn_{0.5}Zn_{0.5}Fe_2O_4$ sample [27]. This size estimation is visually illustrated in Fig 5(d) and graphically presented in the bar diagram shown in Fig 5(e). Table 1 displays the calculated particle size made with the Image J Viewer programme.
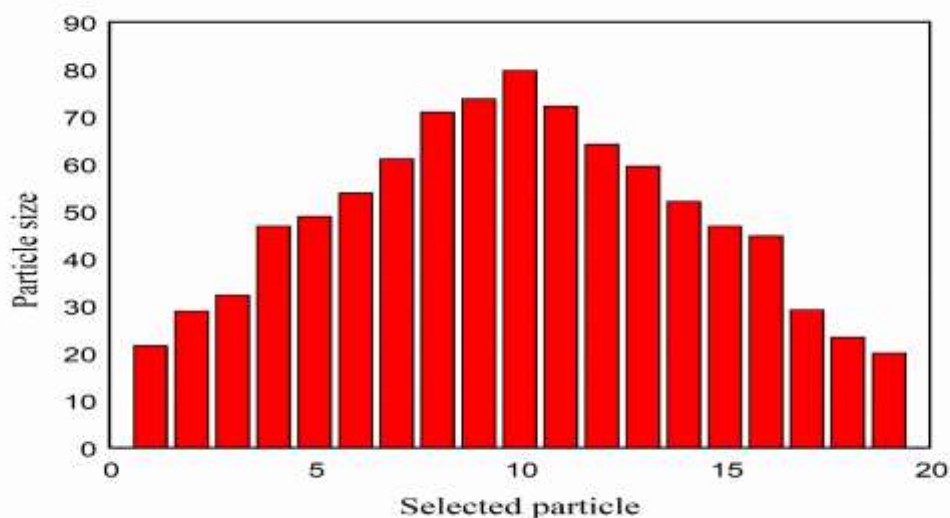

Fig 5(e). Average particle size of HR-TEM by using image 'j' viewer software

104

Eur. Chem. Bull. 2022, 11 (01), 96 – 115

Comprehensive Characterization and Electrochemical Analysis of Zinc-Doped Manganese Ferrite Nanoparticles: Potential for Supercapacitor Applications

Section A-Research paper

Number of particles	Particle size	Number of particles	Particle size
1	21.541	2	28.844
3	32.249	4	46.819
5	48.826	6	53.814
7	61.057	8	70.88
9	73.705	10	79.699
11	72.111	12	64.125
13	59.464	14	52
15	46.819	16	44.721
17	29.12	18	23.324
19	20	**Average**	**48.09**

Table 1. Number of particles and particle size calculated using image 'j' viewer software for $Mn_{0.5}Zn_{0.5}Fe_2O_4$ from HR-TEM

3.6 Energy Dispersive X-Ray Analysis (EDX):

The Energy Dispersive X-ray Spectroscopy examination was carried out at room temperature, and the results are shown in Fig 6. This analysis was conducted to examine the elemental composition of the sample and confirm its purity.
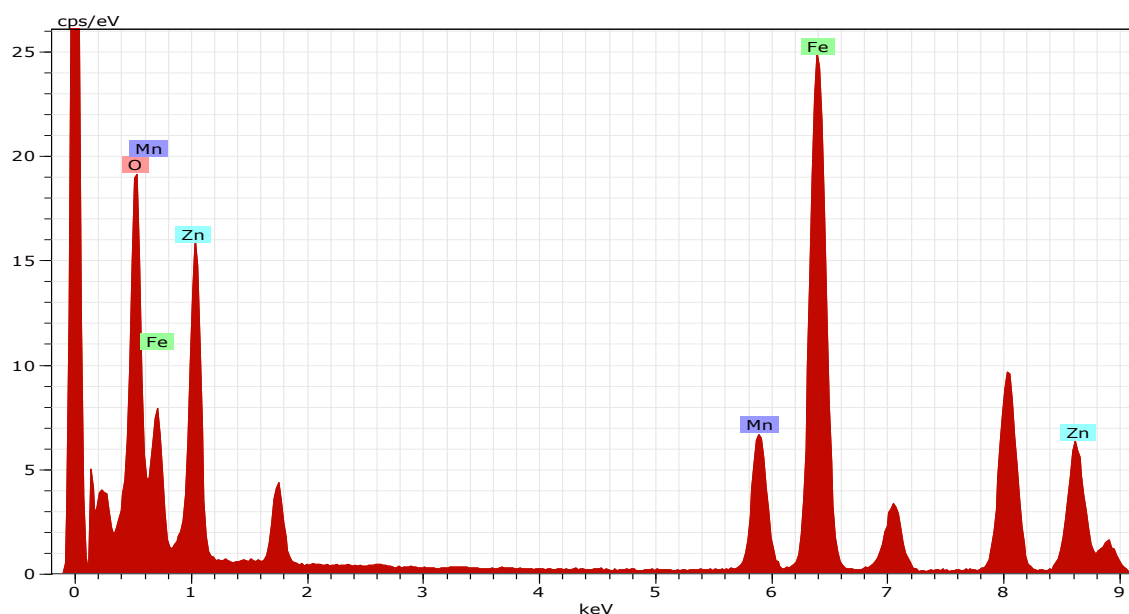

Fig 6 EDX image of $Mn_{0.5}Zn_{0.5}Fe_2O_4$

An EDX spectra display peaks that validate the presence of Mn, Zn, Fe, and O elements in the sample, with no indication of any other impurities [28]. These peaks serve as

105

Comprehensive Characterization and Electrochemical Analysis of Zinc-Doped Manganese Ferrite Nanoparticles: Potential for Supercapacitor Applications

Section A-Research paper

confirmation of the presence of zinc-doped manganese ferrite nanoparticles. Detailed elemental analysis results can be found in Table 2.

Element	Series	Net	unn. C	norm. C	Atom. C	Error(3 sigma)
			[wt.%]	[wt.%]	[at.%]	[wt.%]
Oxygen	K-series	23414	25.06	25.06	54.64	2.38
Iron	K-series	59875	46.35	46.35	28.96	4.29
Manganese	K-series	15101	11.33	11.33	7.19	1.14
Zinc	K-series	16932	17.26	17.26	9.21	1.69
		Total	100.00	100.00	100.00	

Table 2: Elemental analysis of $Mn_{0.5}Zn_{0.5}Fe_2O_4$
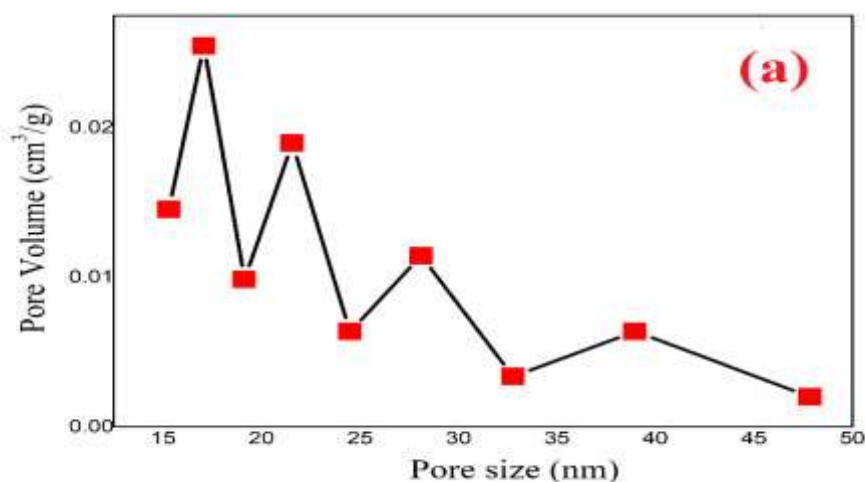
3.7 Brunauer - Emmett - Teller (BET):

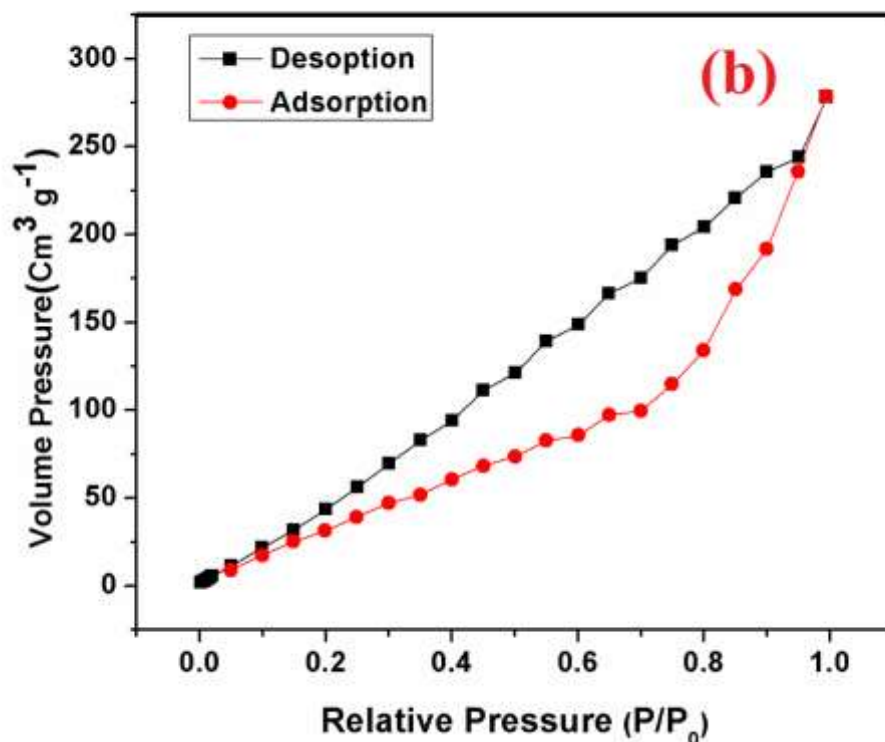**Fig 7(a). Pore distribution of $Mn_{0.5}Zn_{0.5}Fe_2O_4$**

106

Eur. Chem. Bull. 2022, 11 (01), 96 – 115

Comprehensive Characterization and Electrochemical Analysis of Zinc-Doped Manganese Ferrite Nanoparticles: Potential for Supercapacitor Applications

Section A-Research paper

Fig 7(b). N_2 adsorption- desorption isotherm

The pore size distribution curve and a typical N_2 adsorption-desorption isotherm of the $Mn_{0.5}Zn_{0.5}Fe_2O_4$ are shown in Fig 7(a), (b) respectively. As can be seen there is a dominant pore size of 3.41 nm in this region, with a broad mesopore size variation in the 2–15 nm range. This leads us to the conclusion that the porosity structure in this sample is disordered. According to the IUPAC, Fig 7(b) demonstrates that the adsorption isotherm at relative pressure (P/P_0) between 0.0 and 1.0 is IV-type with a type H_2 hysteresis loop. It is believed that the presence of mesopores amid sample is what causes the isotherm to have a pronounced hysteresis loop. The findings of the analysis of nitrogen adsorption show that $Mn_{0.5}Zn_{0.5}Fe_2O_4$ has a BET surface area of 63.6 m^2g^{-1}, which is much greater than the previously reported results for pure sample nanoparticles [29]. These findings implies the $Mn_{0.5}Zn_{0.5}Fe_2O_4$ surface has the more active sites which promotes the supercapacitance behavior of the mesoporous structured synthesized $Mn_{0.5}Zn_{0.5}Fe_2O_4$.
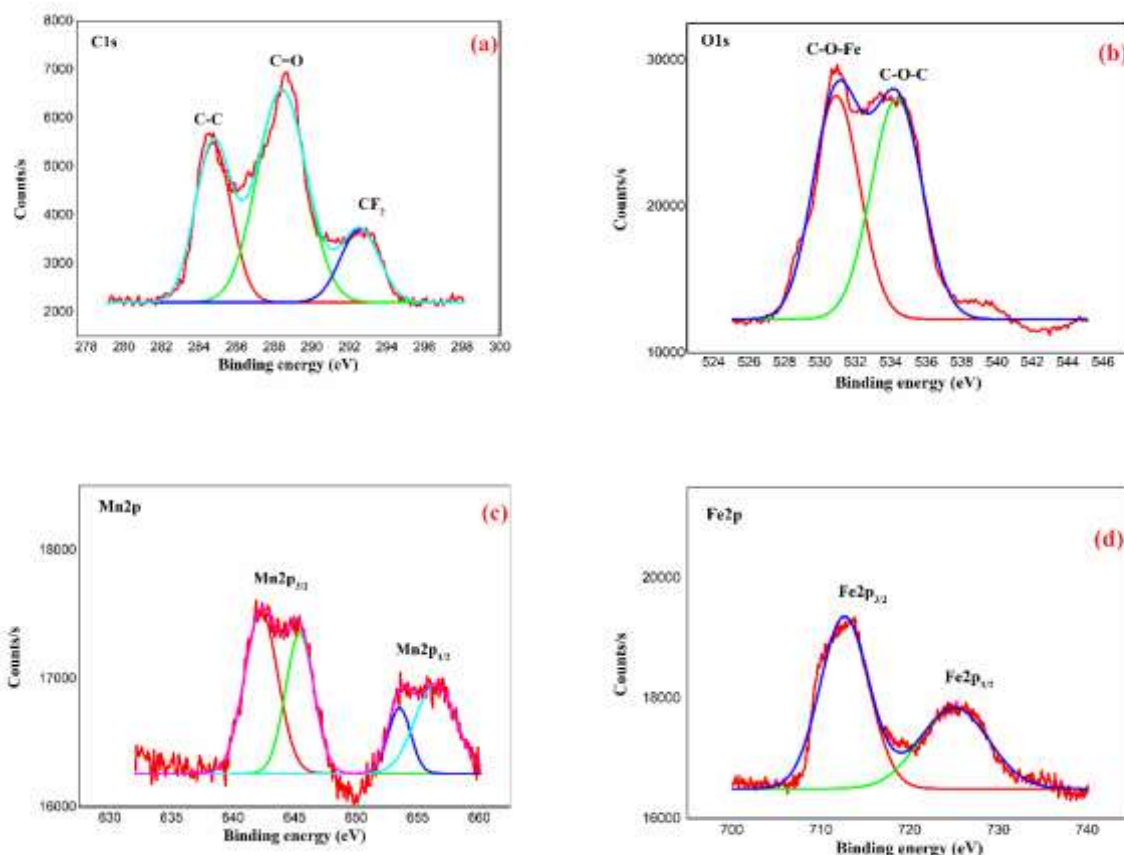
3.8 X-ray Photoelectron Spectroscopy (XPS):

X-ray Photoelectron Spectroscopy analysis plays a vital role in accurately determining the surface components and compositions of a sample. Fig 8(f) illustrates the wide scan XPS spectra of the sample, covering a binding energy range of 0-1200 eV. To measure the binding energies of the individual components in the composite sample, C1s (C-C), (C=O), CF_2 (30),(31),(32) was used as a reference point (approximately 288 eV), as depicted in Fig 8(a). To further validate the presence of each component in the composites, specific XPS spectra were obtained for Oxygen (O1s) (C-O-Fe), (C-O-C) [33], Manganese ($Mn2p_{3/2}$ and $Mn2p_{1/2}$) [34], Ferrous ($Fe2p_{3/2}$ and $Fe2p_{1/2}$) [35], and Zinc ($Zn2p_{3/2}$ and $Zn2p_{1/2}$) [36]. These

107

Comprehensive Characterization and Electrochemical Analysis of Zinc-Doped Manganese Ferrite Nanoparticles: Potential for Supercapacitor Applications

Section A-Research paper

individual XPS spectra, displayed in Fig 8(a) to (e), provide detailed insights into the chemical states and compositions of each respective component within the sample.

The wide scan XPS spectra of the sample are depicted in Fig 8(f), showing the assigned binding energies for different elements. Fig 8(a) specifically displays the binding energy assigned to C1s. The O1s binding energy is illustrated in Fig 8(b), while Fig 8(c) represents the Mn2p binding energy. Additionally, Fig 8(d) exhibits the Fe2p binding energy on the surface of Fe, including the presence of Mn-ZnO and doped Mn with Fe in the sample (Fe-Mn/ZnO). These spectra provide valuable insights into the elemental composition and surface properties of the analyzed sample. The binding energies for the individual components, including C1s, O1s, Mn2p, Fe2p, and Zn2p, have been compiled and presented in Table 3.

The binding energies of Zn2p and Zn2p1 components in the sample were measured to be 1021.5 eV and 1046.5 eV, respectively, as indicated in Fig 8(e) and Table 3. While the FWHM values for each spin-orbit component are similar, the Zn2p and Zn2p1 components exhibit broader peaks compared to Fe2p. This broadening can be attributed to the Coster-Kronig effect, which involves post-ionization processes. Additionally, it is noteworthy that the Zn2p1 peak appears shorter in height compared to the Zn2p peak. The XPS analysis confirms the presence of Mn^{2+} and Fe^{2+} on the surface of the Fe-doped Mn-ZnO sample (Fe-Mn/ZnO), supporting the findings reported in [37].

108

Eur. Chem. Bull. 2022, 11 (01), 96 – 115

Comprehensive Characterization and Electrochemical Analysis of Zinc-Doped Manganese Ferrite Nanoparticles: Potential for Supercapacitor Applications
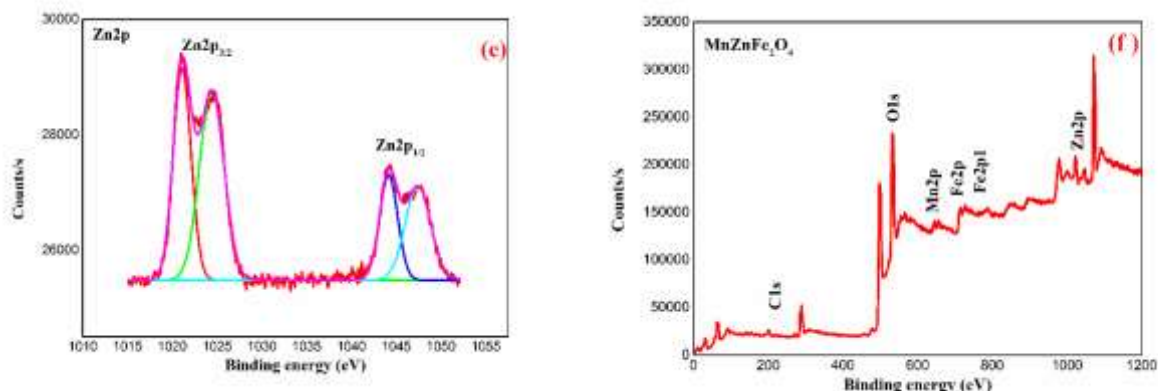
Section A-Research paper

Fig 8 (a), (b), (c), (d) and (e) Deconvolution XPS spectra of c1s, O1s, Mn2p, Fe2p and Zn2p peak of the sample respectively and Fig 8(f) shows wide scan XPS spectra of $Mn_{0.5}Zn_{0.5}Fe_2O_4$ sample

Name	Peak BE	FWHM eV	Area (P) CPS.eV	Atomic %
C1s	288.53	2.33	26519.49	5.28
O1s	532.14	6.37	116424.43	9.57
Mn2p	644.55	6.31	13575.79	0.29
Fe2p	712.99	7.33	41210.79	0.80
Zn2p	1021.66	3.64	33731.78	0.42
Zn2p1	1046.80	5.80	64841.60	2.57

Table 3. Binding Energies of O1s, C1s, Mn2p, and Fe2p components in the synthesized sample.

3.9 Cyclic Voltammetry:

Cyclic Voltammetry was employed to analyze the supercapacitor behaviour of the $Mn_{0.5}Zn_{0.5}Fe_2O_4$ ferrite nano-composite annealed at 700°C. Fig 9 displays the recorded CV curve of the $Mn_{0.5}Zn_{0.5}Fe_2O_4$ electrode at scan rates of 2, 5, and 10 mVs^{-1}. The cyclic voltammogram graph demonstrates a direct association between the voltammetric current and the scan rate, with the current gradually increasing as the scan rate increases. Furthermore,

109

Comprehensive Characterization and Electrochemical Analysis of Zinc-Doped Manganese Ferrite Nanoparticles: Potential for Supercapacitor Applications

Section A-Research paper

the presence of pseudocapacitance in the as-synthesized sample contributes to the broad peak observed alongside the rectangular-shaped cyclic voltammetry. This characteristic rectangular shape of the CV curves suggests a reversible and facile oxidation-reduction process [38].
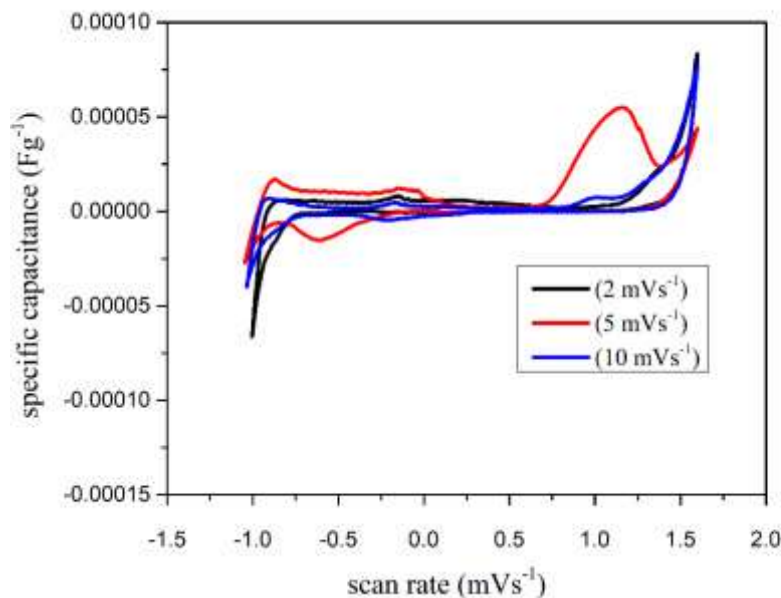

Fig 9. CV pattern of $Mn_{0.5}Zn_{0.5}Fe_2O_4$

The specific capacitance (Cs) value of the Zinc-doped manganese ferrite electrode was calculated using the equation [39]:

$$C_s = \frac{Q}{\Delta v.m}$$

Here, Cs represents the specific capacitance, Q is the combined anodic and cathodic charges obtained during each scanning, m denotes the mass of the electrode material in milligrams (mg), and ΔV indicates the fixed scan rate in millivolts per second (mVs^{-1}). The electrochemical measurements were conducted using a standard three-electrode setup, consisting of a working electrode (the sample), a reference electrode (Ag/AgCl), and a counter electrode (a high platinum wire). The measurements were carried out in the presence of a 0.2 M solution of tetra-butyl ammonium perchlorate [40].

At a lower scan rate of 2 mVs^{-1}, the cyclic voltammetry (CV) investigation found a higher specific capacitance value of 388.35 Fg^{-1}, while a lower capacitance value of 146.24 Fg^{-1} was found at a higher scan rate of 10 mVs^{-1}. This behaviour can be attributed to the ion diffusion process. At lower scan rates, there is ample time for ions to diffuse throughout both the inner and outer regions of the electrode material, resulting in a higher capacitance. Conversely, at higher scan rates, ion diffusion mainly occurs on the external surface of the electrodes, leading to a lower capacitance value [41]. The improved crystallinity of the zinc-doped manganese ferrite nanoparticles is demonstrated by the greater specific capacitance value found at the lower scan rate. This suggests that the nanoparticles possess favourable structural characteristics for enhanced energy storage capabilities.

110

Eur. Chem. Bull. 2022, 11 (01), 96 – 115

Comprehensive Characterization and Electrochemical Analysis of Zinc-Doped Manganese Ferrite Nanoparticles: Potential for Supercapacitor Applications

Section A-Research paper

According to a study by A. Ghasemi *et al.,* the specific capacitance value obtained for a scan rate of 2 mVs^{-1} was reported as 71 Fg^{-1}. However, when comparing this result with the present work on zinc-doped manganese ferrite, the specific capacitance value of 388.35 Fg^{-1} at the same scan rate demonstrates significantly improved suitability for supercapacitor applications [42]. In the research conducted by Mustafa Aghazadeb *et al.,* it was observed that the specific capacitance values for $MnFe_3O_4$ at scan rates of 2 mVs^{-1} and 5 mVs^{-1} were 225 Fg^{-1} and 199 Fg^{-1}, respectively. Comparing these results with the findings of the present study on $Mn_{0.5}Zn_{0.5}Fe_2O_4$, it was found that the specific capacitance values at the same scan rates were significantly higher, measuring 388.35 Fg^{-1}, and 261.72 Fg^{-1} respectively. These findings suggest the superior suitability of $Mn_{0.5}Zn_{0.5}Fe_2O_4$ for supercapacitor applications [43]. As the scan rate was increased from 2 to 10, the specific capacitance values changed. This variation is shown in Fig 9 and summarised in Table 4.

Scan rate (mVs^{-1})	Specific Capacitance (Fg^{-1})
2	388.35
5	261.72
10	146.24

Table 4. Specific Capacitance value of $Mn_{0.5}Zn_{0.5}Fe_2O_4$ (700℃) at different scan rate

Conclusion:

In summary, zinc-doped manganese ferrite ($Mn_{0.5}Zn_{0.5}Fe_2O_4$) nanoparticles were successfully obtained via the co-precipitation technique, and they were then heated to 700°C for annealing. The XRD analysis confirmed the synthesised sample's crystallinity, and the average particle size was estimated to be around 50 nm. The SEM and HR-TEM images showed that the zinc-doped manganese ferrite nanoparticles exhibited a spherical shape. EDX analysis confirmed the presence of Mn, Zn, Fe, and O elements in the sample. Importantly, the cyclic voltammetry study demonstrated a high specific capacitance value of 388.35 Fg^{-1} at a scan rate of 2 mVs^{-1}, indicating the promising suitability of these nanoparticles for supercapacitor applications.

Reference

1. Azadmanjiri, J., 2007. Preparation of Mn–Zn ferrite nanoparticles from chemical sol–gel combustion method and the magnetic properties after sintering. Journal of Non-Crystalline Solids, 353(44-46), pp.4170-4173.
2. Kooti, M. and Sedeh, A.N., 2012. Glycine-assisted fabrication of zinc and manganese ferrite nanoparticles. *Scientia Iranica*, *19*(3), pp.930-933.
3. Khorramdin, A., Shokrollahi, H., Pezeshki, A., Mirzaei, F. and Nader, N.D., 2014. Firooz Salehpour. *Journal of Nanotechnology*, *5*, pp.041002-1
4. Tangcharoen, T., Ruangphanit, A. and Pecharapa, W., 2013. Structural and magnetic properties of nanocrystalline zinc-doped metal ferrites (metal= Ni; Mn;

111

Eur. Chem. Bull. 2022, 11 (01), 96 – 115

Comprehensive Characterization and Electrochemical Analysis of Zinc-Doped Manganese Ferrite Nanoparticles: Potential for Supercapacitor Applications

Section A-Research paper

Cu) prepared by sol–gel combustion method. *Ceramics International*, *39*, pp.S239-S243.

5. Sheikh, A. and Jain, P., 2016. A thorough study of zinc ferrite nanoparticles with reference to green synthesis. *Int J Nanomed Nanosurg*, *2*(3).

6. Devi, E.C. and Soibam, I., 2017. Effect of Zn doping on the structural, electrical and magnetic properties of $MnFe_2O_4$ nanoparticles. *Indian Journal of Physics*, *91*(8), pp.861-867.

7. Angadi, V.J., Manjunatha, K., Praveena, K., Pattar, V.K., Fernandes, B.J., Manjunatha, S.O., Husain, J., Angadi, S.V., Horakeri, L.D. and Ramesh, K.P., 2021. Magnetic properties of larger ionic radii samarium and gadalonium doped manganese zinc ferrite nanoparticles prepared by solution combustion method. *Journal of Magnetism and Magnetic Materials*, *529*, p.167899.

8. Hu, P., Yang, H.B., Pan, D.A., Wang, H., Tian, J.J., Zhang, S.G., Wang, X.F. and Volinsky, A.A., 2010. Heat treatment effects on microstructure and magnetic properties of Mn–Zn ferrite powders. *Journal of Magnetism and Magnetic Materials*, *322*(1), pp.173-177.

9. Ichikawa, R.U., Yoshito, W.K., Saeki, M.J., Maranhão, W.C., Goulart, F. and Martinez, L.G., 2017, August. Characterization of Mn0. 67Zn0. 33Fe2O4 Nanoparticles Synthesized under Different pH. In *Materials Science Forum* (Vol. 899, pp. 48-53). Trans Tech Publications Ltd.

10. Andhare, D.D., Patade, S.R., Kounsalye, J.S. and Jadhav, K.M., 2020. Effect of Zn doping on structural, magnetic and optical properties of cobalt ferrite nanoparticles synthesized via. Co-precipitation method. *Physica B: Condensed Matter*, *583*, p.412051.

11. Waqas, H. and Qureshi, A., 2009. Influence of pH on nanosized Mn–Zn ferrite synthesized by sol–gel auto combustion process. *Journal of Thermal Analysis and Calorimetry*, *98*(2), pp.355-360.

12. Chitra, S.R., Sendhilnathan, S., Gayathri, V. and Sivakumar, M., 2016. Experimental studies from FT-IR with TG-DTA analysis of ferrites. *World Review of Science, Technology and Sustainable Development*, *12*(4), pp.287-299.

13. Arulmurugan, R., Vaidyanathan, G., Sendhilnathan, S. and Jeyadevan, B., 2006. Mn–Zn ferrite nanoparticles for ferrofluid preparation: study on thermal–magnetic properties. *Journal of magnetism and magnetic materials*, *298*(2), pp.83-94.

14. Töpfer, J. and Angermann, A., 2011. Nanocrystalline magnetite and Mn–Zn ferrite particles via the polyol process: Synthesis and magnetic properties. *Materials Chemistry and Physics*, *129*(1-2), pp.337-342.

15. Debnath, S., Deb, K., Saha, B. and Das, R., 2019. X-ray diffraction analysis for the determination of elastic properties of zinc-doped manganese spinel ferrite nanocrystals ($Mn_{0.75}Zn_{0.25}Fe_2O_4$), along with the determination of ionic radii, bond lengths, and hopping lengths. *Journal of Physics and Chemistry of Solids*, *134*, pp.105-114.

16. Amulya, M.S., Nagaswarupa, H.P., Kumar, M.A., Ravikumar, C.R. and Kusuma, K.B., 2021. Sonochemical synthesis of $MnFe_2O_4$ nanoparticles and their

112

Eur. Chem. Bull. 2022, 11 (01), 96 – 115

Comprehensive Characterization and Electrochemical Analysis of Zinc-Doped Manganese Ferrite Nanoparticles: Potential for Supercapacitor Applications

Section A-Research paper

electrochemical and photocatalytic properties. *Journal of Physics and Chemistry of Solids*, *148*, p.109661.

17. Vignesh, V., Subramani, K., Sathish, M. and Navamathavan, R., 2018. Electrochemical investigation of manganese ferrites prepared via a facile synthesis route for supercapacitor applications. *Colloids and Surfaces A: Physicochemical and Engineering Aspects*, *538*, pp.668-677.

18. Ramadan, R., Uskoković, V. and El-Masry, M.M., 2023. Triphasic $CoFe_2O_4/ZnFe_2O_4/CuFe_2O_4$ nanocomposite for water treatment applications. *Journal of Alloys and Compounds*, *954*, p.170040.

19. Ranjith Kumar, E., Arunkumar, T. and Prakash, T., 2015. Heat treatment effects on structural and dielectric properties of Mn substituted $CuFe_2O_4$ and $ZnFe_2O_4$ nanoparticles. *Superlattices and Microstructures*, *85*, pp.530-535.

20. Angermann, A., Töpfer, J., Da Silva, K.L. and Becker, K.D., 2010. Nanocrystalline Mn–Zn ferrites from mixed oxalates: synthesis, stability and magnetic properties. *Journal of alloys and compounds*, *508*(2), pp.433-439.

21. Thakur, P., Sharma, R., Sharma, V. and Sharma, P., 2017. Structural and optical properties of $Mn_{0.5}Zn_{0.5}Fe_2O_4$ nano ferrites: effect of sintering temperature. *Materials Chemistry and Physics*, *193*, pp.285-289.

22. Al-Hada, N.M., Kamari, H.M., Shaari, A.H. and Saion, E., 2019. Fabrication and characterization of Manganese–Zinc Ferrite nanoparticles produced utilizing heat treatment technique. *Results in Physics*, *12*, pp.1821-1825.

23. Al-Hada, N.M., Saion, E.B., Shaari, A.H., Kamarudin, M.A., Flaifel, M.H., Ahmad, S.H. and Gene, S.A., 2014. A facile thermal-treatment route to synthesize ZnO nanosheets and effect of calcination temperature. *PloS one*, *9*(8), p.e103134.

24. Manohar, A., Vijayakanth, V., Vattikuti, S.P. and Kim, K.H., 2023. Structural and electrochemical properties of mixed calcium-zinc spinel ferrites nanoparticles. *Ceramics International*, *49*(3), pp.4365-4371.

25. Kumar, E.R., Jayaprakash, R. and Kumar, S., 2014. The role of annealing temperature and bio template (egg white) on the structural, morphological and magnetic properties of manganese substituted MFe_2O_4 (M= Zn, Cu, Ni, Co) nanoparticles. *Journal of magnetism and magnetic materials*, *351*, pp.70-75.

26. Sagayaraj, R., Aravazhi, S., Praveen, P. and Chandrasekaran, G., 2018. Structural, morphological and magnetic characters of PVP coated $ZnFe_2O_4$ nanoparticles. *Journal of Materials Science: Materials in Electronics*, *29*, pp.2151-2158.

27. Venkatesh, M., Kumar, G.S., Viji, S., Karthi, S. and Girija, E.K., 2016. Microwave assisted combustion synthesis and characterization of nickel ferrite nanoplatelets. *Modern Electronic Materials*, *2*(3), pp.74-78.

28. Debnath, S. and Das, R., 2020. Study of the optical properties of Zn doped Mn spinel ferrite nanocrystals shows multiple emission peaks in the visible range–a promising soft ferrite nanomaterial for deep blue LED. *Journal of Molecular Structure*, *1199*, p.127044.

113

Eur. Chem. Bull. 2022, 11 (01), 96 – 115

Comprehensive Characterization and Electrochemical Analysis of Zinc-Doped Manganese Ferrite Nanoparticles: Potential for Supercapacitor Applications

Section A-Research paper

29. Bhowmik, K.L., Debnath, A., Nath, R.K., Das, S., Chattopadhyay, K.K. and Saha, B., 2016. Synthesis and characterization of mixed phase manganese ferrite and hausmannite magnetic nanoparticle as potential adsorbent for methyl orange from aqueous media: artificial neural network modeling. *Journal of Molecular Liquids*, *219*, pp.1010-1022.

30. Oswald, S., 2015. Binding energy referencing for XPS in alkali metal-based battery materials research (I): Basic model investigations. *Applied Surface Science*, *351*, pp.492-503

31. Fujimoto, A., Yamada, Y., Koinuma, M. and Sato, S., 2016. Origins of sp3C peaks in C1s X-ray photoelectron spectra of carbon materials. *Analytical chemistry*, *88*(12), pp.6110-6114.

32. Dolgov, A., Lopaev, D., Lee, C.J., Zoethout, E., Medvedev, V., Yakushev, O. and Bijkerk, F., 2015. Characterization of carbon contamination under ion and hot atom bombardment in a tin-plasma extreme ultraviolet light source. *Applied surface science*, *353*, pp.708-713.

33. Li, L., Ma, P., Hussain, S., Jia, L., Lin, D., Yin, X., Lin, Y., Cheng, Z. and Wang, L., 2019. FeS 2/carbon hybrids on carbon cloth: a highly efficient and stable counter electrode for dye-sensitized solar cells. *Sustainable Energy & Fuels*, *3*(7), pp.1749-1756.

34. Arasi, S.E., Ranjithkumar, R., Devendran, P., Krishnakumar, M. and Arivarasan, A., 2021. Investigation on electrochemical behaviour of manganese vanadate nanopebbles as potential electrode material for supercapacitors. *Journal of Alloys and Compounds*, *857*, p.157628.

35. Li, Z., Chen, H. and Liu, W., 2018. Full-spectrum photocatalytic activity of ZnO/CuO/ZnFe2O4 nanocomposite as a photofenton-like catalyst. *Catalysts*, *8*(11), p.557.

36. Xu, D., Fan, D. and Shen, W., 2013. Catalyst-free direct vapor-phase growth of Zn 1− x Cu x O micro-cross structures and their optical properties. *Nanoscale research letters*, *8*, pp.1-9.

37. Li, M., Fang, H., Li, H., Zhao, Y., Li, T., Pang, H., Tang, J. and Liu, X., 2017. Synthesis and characterization of MnZn ferrite nanoparticles with improved saturation magnetization. *Journal of Superconductivity and Novel Magnetism*, *30*, pp.2275-2281.

38. Uke, S.J., Mardikar, S.P., Bambole, D.R., Kumar, Y. and Chaudhari, G.N., 2020. Sol-gel citrate synthesized Zn doped $MgFe_2O_4$ nanocrystals: a promising supercapacitor electrode material. *Materials Science for Energy Technologies*, *3*, pp.446-455.

39. Sathiyamurthy, K., Rajeevgandhi, C., Guganathan, L., Bharanidharan, S. and Savithiri, S., 2021. Enhancement of magnetic, supercapacitor applications and theoretical approach on cobalt-doped zinc ferrite nanocomposites. *Journal of Materials Science: Materials in Electronics*, *32*, pp.11593-11606.

114

Eur. Chem. Bull. 2022, 11 (01), 96 – 115

Comprehensive Characterization and Electrochemical Analysis of Zinc-Doped Manganese Ferrite Nanoparticles: Potential for Supercapacitor Applications

Section A-Research paper

40. Pang, S.C., Wee, B.H. and Chin, S.F., 2011. The capacitive behaviors of manganese dioxide thin-film electrochemical capacitor prototypes. *International Journal of Electrochemistry*, *2011*.

41. Hajasharif, P., Ramesh, K., Sivakumar, S. and Sivagurunathan, P., 2019. Synthesis and characterization of copper doped lithium ferrite nanocomposite. *Int. J. Innov. Technol. Explor Eng.(IJITEE)*, *9*(2), pp.33-37.

42. Ghasemi, A., Kheirmand, M. and Heli, H., 2019. A study on the supercapacitive behavior of zinc substituted manganese ferrite nanoparticles. *Journal of the Iranian Chemical Society*, *16*, pp.841-849.

43. Aghazadeh, M., Karimzadeh, I., Ganjali, M.R. and Behzad, A., 2017. Mn 2+-doped Fe_3O_4 nanoparticles: a novel preparation method, structural, magnetic and electrochemical characterizations. *Journal of Materials Science: Materials in Electronics*, *28*, pp.18121-18129.

115

Eur. Chem. Bull. 2022, 11 (01), 96 – 115